Effects of Pairwise, Self-Associating Functional Side Groups on Polymer Solubility, Solution Viscosity, and Mist Control

R. L. Ameri David,[†] Ming-Hsin Wei,[†] David Liu,[†] Brett F. Bathel,[§] Jan P. Plog,[||] Albert Ratner,[‡] and Julia A. Kornfield*,[†]

Division of Chemistry and Chemical Engineering, California Institute of Technology, Pasadena, California 91125; Department of Mechanical and Industrial Engineering, University of Iowa, Iowa City, Iowa 52242; NASA Langley Research Center, Hampton, Virginia 23681; and Thermo Fisher Scientific, 76227 Karlsruhe, Germany

Received September 9, 2008; Revised Manuscript Received December 15, 2008

ABSTRACT: Solution properties are reported for homologous series of narrowly distributed polymers with systematically varied content of self-associating groups. Anionically polymerized polybutadienes of two lengths (510 and 1250 kg/mol) serve as prepolymers that are modified by incorporation of carboxylic acid side groups using thiol−ene coupling to pendant vinyl groups. Carboxylic acid groups strongly reduce polymer solubility in hydrocarbon solvents, restricting the extent of functionalization that can be examined in single-phase solutions (e.g., in chlorododecane, functionalization must be kept <1.8 mol % even for the shorter of the two backbones). In the single-phase regime, addition of hydrogen bond "stickers" weakly affects solution viscosity. Even at concentrations that produce overlap at the scale of strand length between stickers, viscosity increases are less than 1 order of magnitude. These controlled studies (using functionalized and unmodified polymer homologues of matched, well-defined length) challenge the pre-existing understanding of the rheology of self-associating polymers. The results indicate that effects of intrachain pairing are important beyond the dilute regime—behavior unaccounted for in earlier experimental and theoretical studies. The implications for mist control of aviation fuel are that self-associating polymers of acceptable solubility in the fuel are not superior to nonassociating polymers even at concentrations several times above overlap.

Introduction

It has been known since the 1960s that low concentrations of very high molar mass polymers (MW $> 10^6$ g/mol) have potent effects on both hydrodynamic drag in turbulent flows and on the breakup of liquid jets and drops. Both effects have long been attributed to polymer elasticity and to increased solution elongational viscosity.[1−4] Turbulent drag reduction can result from the addition of part-per-million levels (as low as 0.02 ppm)[5] of long-chain polymer to a fluid. Extremely successful mist suppression of fluids of low shear viscosity can be achieved with dilute concentrations of linear chains of sufficiently high molecular weight: for instance, polyisobutylene of $(5−10) \times 10^6$ g/mol suppresses atomization of Jet-A fuel at concentrations as low as 50 ppm.[2,6] Consequently, the addition of small quantities of polymer is a widely used technique to control the behavior of liquids in jet breakup, spray atomization, and splashing in technologies ranging from inkjet printing to agricultural spraying. However, ultralong ($\sim 10^7$ g/mol) linear chains able to powerfully influence fluid behavior in extensional flow at dilute concentrations[2,7] undergo scission in turbulent flow or during passage through pumps, mechanically degrading into smaller chains ($\sim 10^6$ g/mol) exhibiting much less potent drag-reduction or mist-suppression ability. (Thus, drag-reduction activity of ultralong polymer additives decreases with distance along a pipe segment,[8] for instance.)

Attempts have been made to design shear-stable chains of molecular weight $\leq 1 \times 10^6$ g/mol that can aggregate (via intermolecular, noncovalent interactions) at low polymer concentrations ($\sim$1000 ppm) into large clusters that are effective mist-control/drag-reducing agents. One important class of associating polymers that have been investigated as potential mist-control/drag-reduction additives is that of linear chains possessing associating hydrogen-bonding functional groups at random positions along their entire length.[9−11] Unfortunately, previous studies of associating linear polymers as rheology modifiers in elongational flow did not examine in a controlled manner the role of molecular variables, such as chain length or associating-group density.

To establish the scientific foundation for utilizing noncovalent interactions in functional polymers that are both resistant to shear degradation and effective mist-control/drag-reducing agents, our group has undertaken studies of linear chains randomly functionalized with *pairwise* associating groups. (Note that this choice precludes the use of, for instance, ionic interactions, which tend to result in multivalent clusters or groupings.) The present study examines carboxylic acid side groups[12] as *self-associating* stickers; a subsequent contribution will report results obtained using acid−base *complementary* associations. Here, two homologous series of well-defined linear polymers (referring to chains of matched length and narrow length distribution, refer to Table 1) were prepared by functionalizing anionically synthesized linear polybutadienes of 510 and 1250 kg/mol to systematically varied extent. Carboxylic acid side groups were incorporated by grafting 3-mercaptopropionic acid to the pendant double bonds of 1,2-units in the polybutadiene chains.[13,14]

The model polymers were subjected to complementary measurements to evaluate the size of the supramolecular aggregates that they form and the consequences those aggregates have on rheological properties and mist suppression. Attention was focused on low-concentration solutions relevant to anti-misting of aviation fuel (a specific engineering objective of our research efforts, motivated by the need to improve the fire safety of aviation fuel in the context of aviation safety and aviation security). Viscosity measurements of entangled solutions were included to test existing theory of the gelation of self-association

* Corresponding author. E-mail: jak@cheme.caltech.edu.
[†] California Institute of Technology.
[‡] University of Iowa.
[§] NASA Langley Research Center.
[||] Thermo Fisher Scientific.

10.1021/ma802058s CCC: $40.75
Published on Web 02/03/2009

Table 1. Reaction Conditions and Results for Polybutadiene Functionalization with 3-Mercaptopropionic Acid

entry[a]	[PB] (g/mL)	[MPA][b]	[AIBN] (mg/mL)	rxn time (h)	funct[c] (%)	PDI[d]	rxn rate[e] ($mL^{3/2}/(mol^{3/2}$ s))
510kPB0.2A	0.016	0.023	0.52	1.2	0.2	1.24	37
510kPB0.3A	0.016	0.021	0.52	2.5	0.3	1.20	30
510kPB1.0A	0.020	0.040	0.65	1.7	1.0	1.23	55
510kPB1.8A[f]	0.018	0.064	0.57	1.8	1.8	1.28	73
510kPB4.7A	0.017	0.13	0.52	1.5	4.7	1.23	130
510kPB7.1A	0.014	0.16	0.49	1.6	7.1	1.28	170
1250kPB0.2A[g]	0.010	12	0.46	0.58	0.2	1.15	41
1250kPB0.3A	0.009	16	0.62	0.55	0.3	1.29	44
1250kPB0.4A	0.009	16	0.52	1.1	0.4	1.17	35
1250kPB0.6A	0.009	16	0.54	1.2	0.6	1.23	43

[a] Functionalized PB polymers were named so that the prefix corresponds to the molecular weight of the precursor chain, and the suffix represents the mole percent of monomers bearing pendent acid groups. [b] In molar equivalent of 1,2-PB units, which are 98% of the units of 510kPB and 8% of the units of 1250kPB. [c] Molar fraction of functionalized monomers based on the total number of PB monomers (both 1,2 and 1,4 units). [d] Reported values correspond to aged samples (12−18 months for 510kPB*xx*A polymers and 6−12 months for 1250kPB*xx*A polymers) and reflect the slow cross-linking of the polymer chains that occurs with time upon storage (see text). The 510kPB and 1250kPB prepolymers had PDI values of 1.15 and 1.09, respectively. [e] Average reaction rate divided by [1,2-PB units][MPA][AIBN]$^{1/2}$. [f] ^{1}H NMR spectrum is shown in Figure 2. [g] GPC trace is given in Figure 3.

polymers. Our specific viscosity results indicate a significant degree of chain collapse which is absent from prior models; therefore, we present a theoretical model of chain size at infinite dilution to gain insight into the role of chain collapse. The body of results presented here calls into question many of the widely accepted conclusions presented in the prior literature (refer to Figures 14 and 15 of the Discussion section). We find that inadequate attention was given to issues of phase separation and to the compact conformations that chains adopt when they are decorated with self-associating stickers.

Experimental Section

Materials. Prepolymer polybutadiene (PB) chains of weight-average molecular weight $M_w = 510$ kg/mol (containing ∼98% 1,2 units and with $M_w/M_n = 1.15$), hereafter referred to as 510kPB, were kindly provided by Dr. Steven Smith of Procter and Gamble Co. Prepolymer PB chains of $M_w = 1250$ kg/mol, hereafter referred to as 1250kPB, were purchased from Polymer Source, Inc. (product ID P1914-Bd, containing ∼8% 1,2 adducts, with $M_w/M_n = 1.09$). Polyisobutylene of $M_w = 4200$ kg/mol, hereafter referred to as 4200kPIB, was purchased from Aldrich (product number 181498, with $M_w/M_n = 1.35$). 2,6-Di-*tert*-butyl-4-methylphenol (BHT), 3-mercaptopropionic acid (MPA), and 2,2′-azobis(2-methylpropionitrile) (AIBN) were obtained at 99% purity from Sigma-Aldrich. AIBN was recrystallized biweekly in methanol (10 mL of solvent per g of AIBN) and stored at 4 °C; all other reagents (as well as solvents) were stored at room temperature and used as received without further purification.

Representative Procedure for PB Functionalization with MPA. To 510kPB (3.6 g, 67 mmol of repeat units) dissolved in 175 mL of tetrahydrofuran (THF) in a 500 mL Schlenk round-bottom flask were added MPA (0.45 g, 4.2 mmol) and AIBN (113 mg, 0.69 mmol) dissolved in 25 mL of THF. The contents of the Schlenk flask were degassed in three freeze−pump−thaw cycles, warmed to 55 °C, and then allowed to react at 55 °C for 105 min. Following the reaction, the polymer solution was transferred to a 500 mL jar containing a small amount of BHT, cooled in liquid nitrogen, and precipitated by addition of 200 mL of cold methanol. The polymer was purified by reprecipitation from a THF solution (containing ca. 1 wt % BHT) with cold methanol, followed by drying to constant weight under vacuum at room temperature. Reaction conditions and results for this example are summarized in Table 1 (entry 510kPB1.8A).

Polymer Characterization. The extent of incorporation of MPA units into PB polymer was determined by analysis of ^{1}H NMR spectra, obtained using a Varian Mercury 300 spectrometer (300 MHz). All spectra were recorded in $CDCl_3$ and referenced to tetramethylsilane. Measurements of polymer molecular weight distributions by gel permeation chromatography (GPC) were carried out in THF at 25 °C eluting at 0.9 mL/min through four PLgel 10-μm analytical columns (Polymer Laboratories, 10^6-10^3 Å in pore size) connected to a Waters 410 differential refractometer detector ($\lambda = 930$ nm). All GPC measurements were analyzed based on calibration using polystyrene standards. Polystyrene-equivalent molecular weights determined in this manner were substantially larger for PB than values provided by the suppliers of the polymers. The latter values, which were obtained by light scattering in conjunction with GPC, are reported above.

Viscosity and Size Measurements. Polymer solutions for viscosity measurements were prepared by combining polymer and solvent in clean 20 mL scintillation vials, which were placed on a Wrist-Action Shaker (Burrell Scientific) for up to 72 h to allow the polymer to dissolve fully and homogenously. For solutions of viscosities ≥10 Pa·s, homogeneity was achieved by first preparing diluted solutions using dichloromethane (DCM) as cosolvent, followed by selective and complete evaporation of the DCM under reduced pressure. (This method was enabled by the >100 °C difference in normal boiling points between DCM and the solvents we used.) Shear viscosity measurements were performed under steady-state flow using an AR1000 rheometer from TA Instruments. The following complementary geometries enabled measurements of viscosities ranging from 10^{-3} to 10^5 Pa·s: (i) an aluminum cone of 60 mm diameter, 1° angle, and 29 μm truncation, (ii) a steel cone of 40 mm diameter, 2° angle, and 55 μm truncation, and (iii) a steel plate of 25 mm diameter.

Polymer samples used for measurements of hydrodynamic diameter by dynamic light scattering were prepared by filtration of dilute polymer solutions through a 0.4 μm pore PTFE membrane with Acrodisc CR 25 mm syringe filters. A ZetaPALS (Brookhaven Instruments Corp.) instrument was used to perform the size measurements. Experiments were carried out using a laser source with wavelength of 532 nm, and the scattered light was collected at an angle of 90°. The built-in Particle Size Software was used to analyze the acquired raw data. Reported apparent hydrodynamic radii represent averages of nine runs of 1 min each.

Characterization of Fluid Breakup and Atomization. The elasticity and relaxation time of polymer solutions under elongational deformation were studied using capillary breakup extensional rheometry using a Thermo Haake CaBER1 instrument. The effect of polymer on drop breakup was characterized using two methods. The first investigates the splashing, spreading, and breakup processes of individual drops impacting a smooth, solid surface. The second experiment involves the spraying of fuel with a simple paint gun (HUSKY Gravity Feed Spray Gun, model HDS 780) and visualizing the resulting spray pattern.

The three methods above are chosen for their complementary advantages and limitations. For the present study, CaBER measurements were restricted to semidilute solutions ($c > c_{min} > c^*$, where $c^* \approx 2500$ ppm by weight for 1250kPB in Jet-A and CaBER failed below 15 000 ppm), and droplet impact only led to breakup for dilute solutions ($c < c_{max} < c^*$; specifically, no breakup occurred for concentrations above 1000 ppm). The only method that is applicable across a wide range of concentrations spanning c^* is the spray experiment. CaBER provides the most quantitative

measurements of effective extensional properties of dilute polymer solutions, but for practical purposes it is limited to the testing of solutions of sufficiently high extensional viscosity[15] (i.e., for Newtonian fluids the shear viscosity must exceed ~ 100 mPa·s; fluids of lower viscosity can only be examined if they have high elasticity, e.g., solutions of linear polymers having $M_w > 10^7$ g/mol). High-speed imaging of drop spreading and breakup generates high deformation rates (>10^3 s^{-1}) and is remarkably reproducible, but analysis is difficult, and for the present polymers, concentrations below 1000 ppm were required to permit breakup. Spray experiments are strictly qualitative, in part because spray patterns on 2-dimensional surfaces vary greatly based on experimental settings such as the position of the gun relative to the surface and the air pressure. The appeal of the method, however, is that it can be used to evaluate in a rapid (although coarse) manner the extent of mist suppression imparted by a polymer additive of *any* molecular weight at *any* concentration in solution.

Capillary breakup rheometry and its application to the measurement of elongational properties of low-viscosity elastic fluids have been established by McKinley and co-workers.[1,15] The CaBER1 system measures the effective extensional properties of a fluid confined to a small column between parallel disks of diameter $D_0 = 4-8$ mm, by first imposing a rapid axial step strain of prescribed magnitude to induce a statically unstable "neck" shape and then by measuring with a laser the thinning and breakup of the resultant filament under the action of capillary forces. Filament thinning, driven by the capillary pressure, is resisted by the extensional stress in the fluid. The principal experimental results obtained are the evolution of the midpoint diameter $D_{mid}(t)$ and the critical time to breakup. The Hencky strain ε_H and the apparent extensional viscosity η_{ext} are determined as follows:

$$\varepsilon_H(t) = 2\ln\left(\frac{D_0}{D_{mid}(t)}\right) \quad (1)$$

$$\eta_{ext}(t) = \frac{\sigma}{-dD_{mid}/dt} \quad (2)$$

where σ is the surface tension. As the fluid filament thins, a window of time in which D_{mid} decays exponentially is typically observed for sufficiently elastic fluids; this regime is used to extract a characteristic relaxation time λ of the fluid ($D_{mid} \sim \exp[-t/3\lambda]$).

Drop impact experiments were done in the laboratory of Prof. Albert Ratner at the University of Iowa, according to methods developed by his group.[16] Droplets of diameter 3 mm were carefully forced out of a needle (one at a time) and allowed to impact a smooth quartz surface at velocities of 3 m/s, while a high-speed, high-resolution camera captured the deformation and breakup behavior at frame rates of 4 kHz and spatial resolution of 15 μm/pixel (Figure 1a). Criteria for characterizing breakup include investigation of the amount of splashing, the amount of fluid ejected, and the survival time of fluid filaments. The latter is most readily quantified and serves as our primary criterion for comparing differently functionalized polymers.

All spray measurements were performed according to the following conditions: Solution aliquots of volume $^1/_2$ mL were sprayed in a fume hood at horizontal angle from a vertical height of 30 cm using 10 psi air pressure, and images of the sedimenting droplet pattern on the bench surface were recorded 80 cm downstream from the spraying source.[17] Spray patterns for solutions of 4200kPIB polymer in Jet-A (Figure 1b) demonstrate that this simple experiment is able to expose the mist-suppressing action of known mist-suppressing materials.

Choice of Solvents. We found that polymer solubility is largely affected by solvent−sticker and sticker−sticker interactions. In order to evaluate the effect of solvent polarity on phase behavior and viscosity, measurements were conducted in dodecane (DD), 1-chlorododecane (CDD), tetrachloroethane (TCE), and chloroform. For the testing of theoretical literature models of self-associating, pairwise interactions, CDD solvent was chosen because it seemed to provide a good trade-off between good polymer solubility and strong interactions (interaction strength increases with decreasing solvent polarity). Given our specific interest in the potential use of self-assembling polymers as low concentration additives for improved mist suppression of aviation fuel, we focused our efforts in the measurement of fluid breakup and atomization (drop impact, spray, and CABER experiments) on polymer solutions in Jet-A.

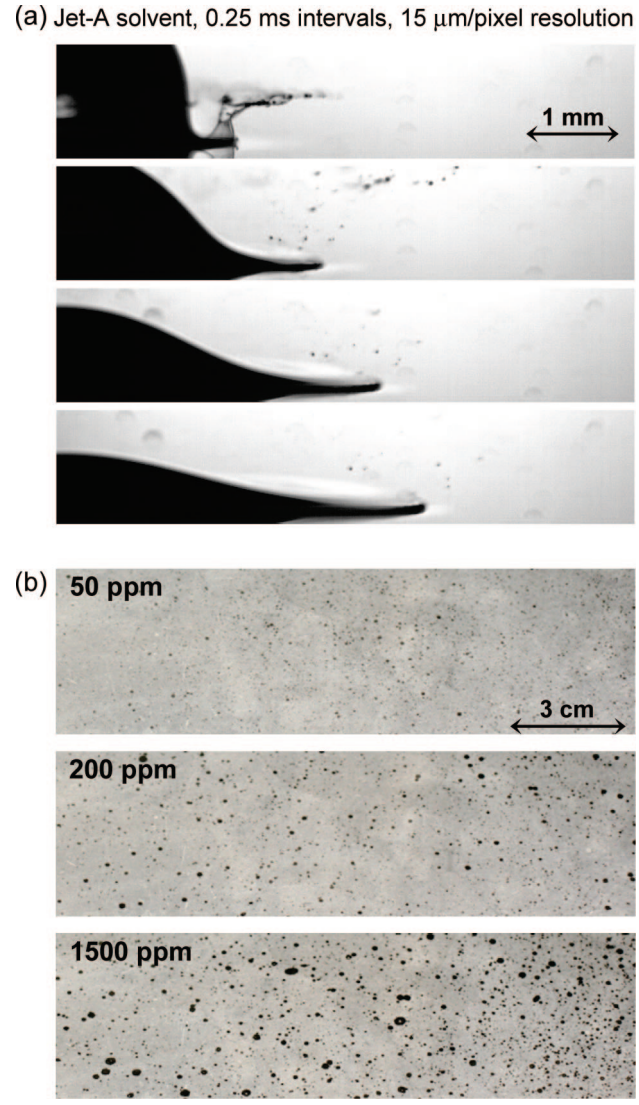

Figure 1. (a) Results of drop splashing, spreading, and breakup for Jet-A solvent. Notice that the ejected fluid breaks up so quickly that only a small number of individual droplets can be resolved after 0.5 ms. (b) Sprays patterns for solutions of 4200 kg/mol polyisobutylene polymer at increasing weight fraction in Jet-A. For reference, pure Jet-A is atomized so finely that there is no observable spray pattern: the fine mist is entrained by the upward air flow of the fume hood and does not settle onto the surface.

Results

Synthesis of Acid-Functionalized Polybutadiene. Reaction of PB prepolymer according to Scheme 1 using reaction conditions summarized in Table 1 allows controlled incorporation of carboxylic acid side groups by radical addition of MPA to the pendant double bonds of 1,2-PB units (Table 1, Figure 2). Consistent with general results for PB modification by thiol−ene coupling under similar conditions,[18] we found that the functionalization reaction occurs with minimal degradation of the precursor material. Because our studies spanned several months, the stability of functionalized polymer over time was investigated. We found that cross-linking occurs slowly (Table

Scheme 1. Synthesis of Acid-Functionalized Derivatives of Polybutadiene Polymers Containing 98% 1,2 Adducts (a) and 8% 1,2 Adducts (b)

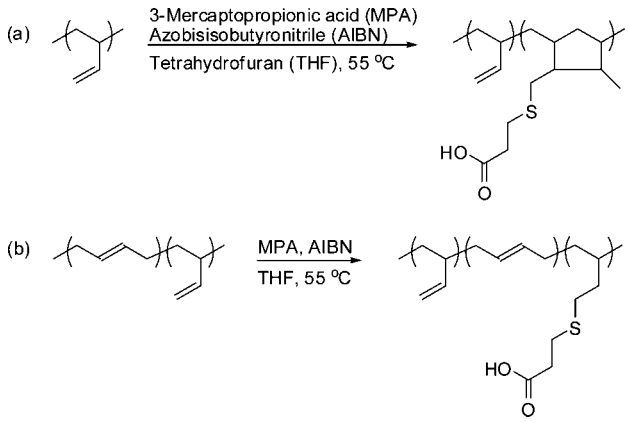

1, Figure 3) but that this process could be minimized by stabilizing the polymer with a small amount of BHT and storing it in the dark below 0 °C. Under these conditions, polymer cross-linking caused M_w/M_n to increase by ~0.1 over time periods of up to 18 months.[19] As an example, the polydispersity of 510kPB0.2A increased from $M_w/M_n \sim 1.16$ after reaction to $M_w/M_n \sim 1.24$ after 18 months, compared with $M_w/M_n \sim 1.15$ for 510kPB prepolymer. We note here that the unexpected behavior presented in this study (see Results and Discussion below) cannot be explained by the small amount of polymer cross-linking described here. That is, cross-linking would increase viscosity and elasticity of polymer samples relative to monodisperse samples, but the results reported here are instead surprisingly small changes of polymer properties as a result of carboxylic acid functionalization.

As documented in a previous publication,[18] possible cyclization of neighboring 1,2-PB adducts (when present) results in

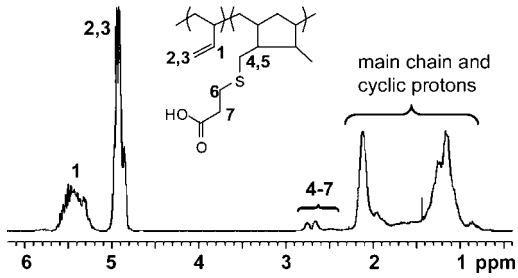

Figure 2. Representative ^{1}H NMR spectrum of acid-functionalized polybutadiene polymer (510kPB1.8A, refer to Table 1). Note that protons 4 and 5 are not equivalent.

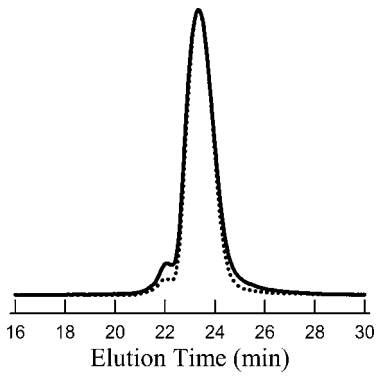

Figure 3. Representative gel permeation chromatography trace of acid-functionalized polybutadiene polymer. The solid line corresponds to 1250kPB0.2A (after 10 months of storage; refer to Table 1); the dashed line is 1250kPB prepolymer.

Table 2. Polymer Solubility as a Function of 3-Mercaptopropionic Acid Content (mol % Monomer Basis) in Various Solvents at Room Temperature

	510k 1, 2-PB[a]		1250k 1, 4-PB[b]	
	1-phase	2-phase	1-phase	2-phase
dodecane	1.0	1.8		0.2
chlorododecane	1.0	1.8	0.6	
Jet-A	1.0	1.8	0.6	
tetrachloroethane	1.8	4.7	0.6	
chloroform	4.7	7.1	0.6	

[a] The polymers with degrees of functionalization reported in the 1-phase column were found to be soluble at all concentrations tested, while the polymers with degrees of functionalization reported in the 2-phase column exhibited phase separation at low concentrations (500−2500 ppm). [b] Four degrees of functionalization were examined for 1250kPB (Table 1): none were soluble at low concentration (500−2500 ppm) in dodecane; all were soluble in the other solvents.

the formation of five-member ring structures, so that in fact the predominant polymer structure arising from functionalization of 1,2-PB chains at low thiol concentration is that shown in Scheme 1a. In other words, the 510kPB chains documented in Table 1 contain roughly the same number of cyclic structures as MPA groups. However, because all of the molecules subjected to further study contained <2% side groups, it seems reasonable to expect that structural changes to the polymer backbone are of little consequence.[20] The extent of MPA incorporation was determined upon analysis of ^{1}H NMR spectra by integration of backbone and side-group peaks, as explained in the Supporting Information. It proved difficult to achieve target levels of functionalization by kinetic control of the reaction due to poor reproducibility of the reaction rates (refer to last column of Table 1). For example, nearly identical reaction conditions were used during synthesis of 1250PB0.6A and 1250PB0.4A. Investigation of the kinetics of the radical functionalization reaction was beyond the scope of this study.

Phase Behavior. Incorporation of carboxylic acid functional groups onto PB chains decreases polymer solubility due to unfavorable solvent−sticker interactions. Intra- and intermolecular polymer associations further drive phase separation of the polymer into a dense phase, which occurs above a maximum MPA content (Table 2) even at low polymer concentrations (500−2500 ppm).

The maximum MPA content that is compatible with polymer solubility increases with increasing solvent polarity (Table 2), consistent with the known decrease in the association strength of carboxylic acids with increasing solvent polarity.[21] The maximum MPA content compatible with single-phase solutions also reflects solvent quality for the polymer backbone. In the least polar solvent (dodecane), the tendency to phase separate as MPA units are added is more severe for 1,4-PB than for 1,2-PB, in accord with the more favorable polymer−solvent interactions for 1,2-PB in *n*-alkanes: C_5-C_8 *n*-alkanes at 60 °C are approximately Θ-solvents for 1,4-PB (the Flory−Huggins interaction parameter is $\chi \sim 0.5-0.6$ for chains of size ~10^4 g/mol), while they are fair solvents for 1,2-PB ($\chi \sim 0.3-0.4$ for chains of comparable size).[22] In addition, the tendency for polymer phase separation was found to be lower in chlorinated or aromatic hydrocarbons (the latter are present at 10−40% in aviation fuels such as Jet-A) than in less polar solvents, consistent with the higher affinity of the polybutadiene backbones for halogenated and aromatic solvents: at 60 °C for both 1,2-PB and 1,4-PB chains of size ~10^4 g/mol, χ values are smaller by about 0.1 for 1-chloropentane compared to *n*-pentane, χ is ~ 0.1 for chloroform, and χ is ~ 0.1−0.2 in toluene.[22] Thus, the observed trends in phase behavior indicate that increasing solvent polarity expands the single-phase region due to the combined effects of increased solubility of the chain backbone and decreased strength of hydrogen bonding.

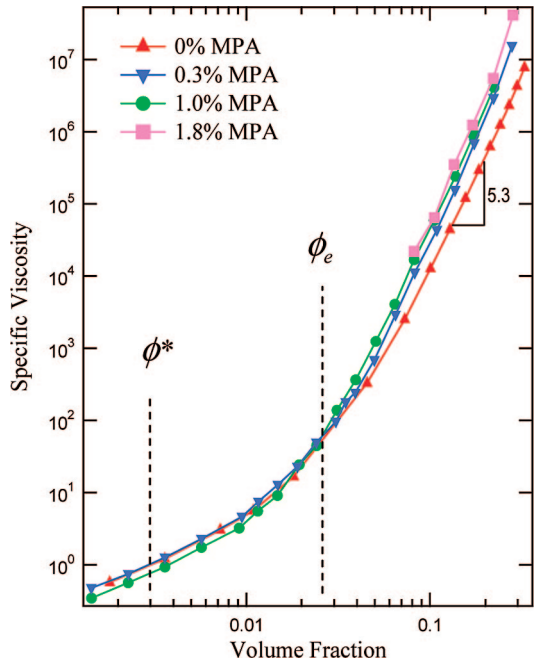

Figure 4. Zero-shear specific viscosity ($\eta_{sp} \equiv \eta_{solution}/\eta_{solvent} - 1$, where $\eta_{solvent} = 2.72$ mPa·s) of 510 kg/mol 1,2-polybutadiene chains in 1-chlorododecane at 20 °C, as a function of 3-mercaptopropionic acid (MPA) content. For 510kPB prepolymer, the overlap concentration corresponds to $\phi^* \cong 0.003$ according to the criterion $[\eta]\phi^* \cong 1$, and the entanglement concentration is $\phi_e \cong 0.026$ (determined as the intersection of the semidilute and entangled regimes, corresponding to $\eta_{sp} \sim \phi^{1.3}$ and $\eta_{sp} \sim \phi^{5.3}$ regimes, respectively). The overlap concentrations of the strands between stickers were determined (using the expression[26] $\phi_s = \phi^*(MW_{chain}/MW_{strand})^{-0.76}$) to be $\phi_s = 0.04$, 0.10, and 0.15 for polymer chains containing 0.3%, 1.0%, and 1.8% MPA side groups, respectively.

Effects of Stickers on Shear Viscosity for Homogeneous Solutions. The magnitude of the effects of stickers on solution shear viscosity was small over the entire range from dilute to entangled concentrations. Even at polymer volume fraction above the overlap of the strands between stickers ϕ_s (such that interchain associations are more probable than intrachain associations), stickers generated enhancements in η_{sp} no larger than 10-fold for all 510 kg/mol 1,2-PB polymer solutions investigated (Figure 4). We were surprised to find such small increases in viscosity, particularly at the highest degrees of functionalization and polymer concentration investigated. Indeed, for 510kPB1.8A polymer at 30 vol % in CDD, polymer concentration is twice ϕ_s, and the strand length between stickers is ~3000 g/mol, leading us to anticipate a dramatic viscosity increase due to the formation of an entangled thermoreversible network. The anticipated[23−25] steep increase in shear viscosity with increasing polymer concentration in the vicinity of ϕ_s, due to the transition from intra- to intermolecular pairing, was not observed.

Stickers cause a decrease in η_{sp} in dilute solutions and an increase in η_{sp} in semidilute solutions, for both 510 kg/mol 1,2-PB chains in CDD (Figure 4, with $\phi^* \cong 0.003$ for the unfunctionalized prepolymer) and 1250 kg/mol 1,4-PB chains in Jet-A (Table 3, with $c^* \sim 0.25$ wt % for the unfunctionalized prepolymer). This result is evidence of the competing effects between intra- and intermolecular interactions. On the one hand, intramolecular associations collapse chains and thereby decrease shear viscosity; this effect is dominant at dilute concentrations. On the other hand, intermolecular associations result in viscosity enhancements, and the magnitude of this effect increases with increasing polymer concentration above the overlap. The crossover of the η_{sp} vs c curves for associating and nonassociating polymer solutions, which depends on the competition between these two opposing effects, was observed to occur in all cases at a polymer concentration substantially greater than the overlap concentration of the unfunctionalized polymer (Figure 4, Table 3).

Table 3. Zero-Shear Specific Viscosity[a] of 1250 kg/mol 1,4-Polybutadiene Chains as a Function of 3-Mercaptopropionic Acid Content and Concentration in Jet-A at 25 °C

c (wt %)	0% A	0.2% A	0.3% A	0.6% A
0.25	1.04	0.99	0.92	0.77
0.5	2.7	3.0	2.8	2.4
1.5	32	42	56	65

[a] $\eta_{sp} \equiv \eta_{solution}/\eta_{solvent} - 1$, where solvent viscosity was 1.45 mPa·s. Measurement reproducibility was typically within 0.03 mPa·s or 3% of the measurement (whichever is greater).

Our attempts to isolate the effects of intramolecular associations on the conformation of individual chains by measuring the viscosity of dilute solutions were not successful. According to the Einstein relationship,[27] the specific viscosity η_{sp} in dilute solution is proportional to the hydrodynamic volume occupied by individual chains, so that the collapse of individual chains can be measured by the ratio of the specific solution viscosities of an associative polymer and its unfunctionalized polymer counterpart at infinite dilution: $\lim_{c\to 0}[r_{n,sp} = (\eta - \eta_{solvent})/(\eta_{ref} - \eta_{solvent})]$. Unfortunately, accurate determination of $r_{\eta,sp}$ was achieved only when $\eta_{sp} > 0.5$ (which required concentrations $>{}^1/_2\phi^*$) using the 60 mm cone-and-plate geometry (which was chosen over a Couette geometry for which measurement accuracy suffered from poorer temperature control).

Effects of solvent and temperature were evaluated in the concentration regime in which stickers increase η_0, using $\phi = 0.10$. With increasing temperature the specific viscosity decreases, as expected, with stickers generally giving a stronger temperature dependence than the unfunctionalized parent polymer (compare 0.3% and 0% MPA polymers in Figure 5; this stronger dependence is attributed to the decreasing strength of H-bonding interactions between carboxylic acid stickers with increasing temperature). Solvent effects accord with qualitative expectations: shifting from a nonpolar solvent (DD) to a slightly polar solvent (CDD) has little effect on the viscosity of solutions of the unfunctionalized polymer and strongly reduces the viscosity of the polymer with 0.3% stickers. The magnitude of solvent effects, however, was somewhat unexpected. For example, the change from DD to CDD results in larger changes in viscosity than the change from CDD to TCE. To place the magnitude of these effects in perspective, note that for 510kPB0.3A the reduction of solution viscosity resulting from changing from DD to CDD is comparable to the reduction of viscosity produced by a 6-fold decrease of sticker content holding solvent fixed (from 510kPB1.8A to 510kPB0.3A in CDD solvent, at both 8 and 20 °C). Evidently, small changes in polarity for nonpolar solvents can be more important than major changes in molecular structure.

On the basis of existing reports of shear thickening in associative polymers,[11,28] we examined the shear rate dependence of the viscosity. Monotonic shear thinning was observed in all but a very few cases, two of which are shown in Figure 6. Thickening was the exception, not the rule, and when it was found, its magnitude was not significant (rising only 20% above the zero-shear viscosity before the onset of shear thinning). The effect was very weak compared to that described in the prior literature (see Discussion below).

Effects of Stickers on Hydrodynamic Size. The observed viscosities indicate that coils adopt more compact configurations as stickers are added (e.g., $r_{\eta,sp} = 0.74$ for 1250kPB0.6A near c^* of the prepolymer in Jet-A; refer to Table 3). Dynamic light scattering measurements were performed to see if they could

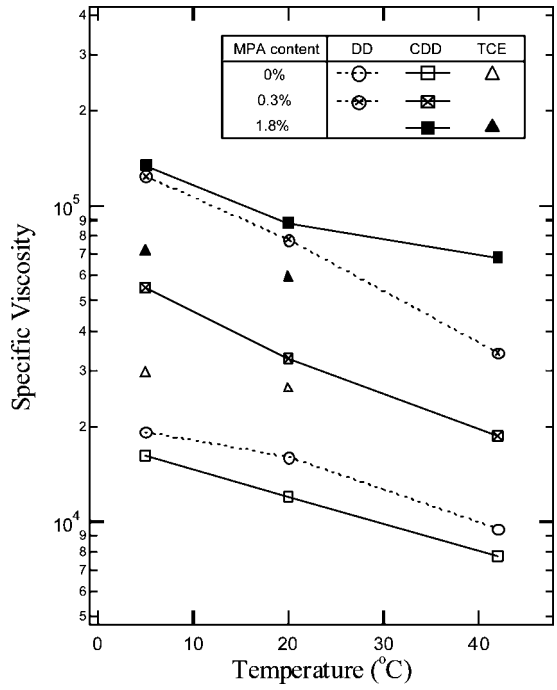

Figure 5. Temperature and solvent effects on specific viscosity ($\eta_{sp} \equiv \eta_{solution}/\eta_{solvent} - 1$) of 10 vol % solutions (in dodecane (DD), chlorododecane (CDD), and tetrachloroethane (TCE) solvents) of 510 kg/mol 1,2-polybutadiene chains as a function of mercaptopropionic acid (MPA) content. Note that experiments in TCE were limited to temperatures ≤20 °C due to solvent volatility and that experiments with 1.8% stickers were not possible in DD due to phase separation.

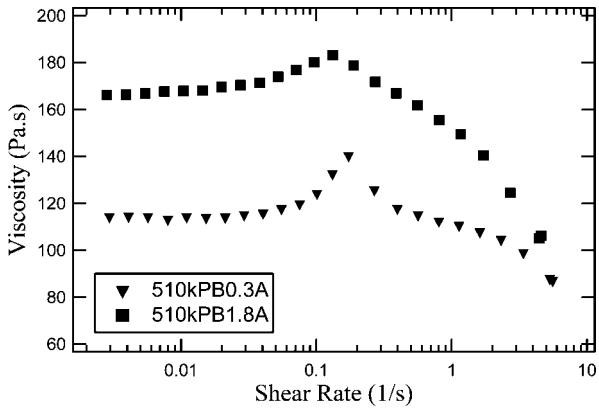

Figure 6. Shear viscosity as a function of shear rate for 10 vol % 510 kg/mol 1,2-polybutadiene solutions in tetrachloroethane at 20 °C.

extend to sufficiently dilute solutions to accurately measure the hydrodynamic radius R_h of single, isolated chains. Unfortunately, we found that measurement sensitivity limited the concentration range to ≥0.05 wt % (∼c^*/5 based on unmodified 1250kPB in Jet-A). This was not sufficiently dilute to reach the single-chain limit: as shown in Table 4, a significant concentration dependence remains, indicating that interchain hydrogen bonding contributes (making the apparent hydrodynamic size greater than that of a single chain).

Modeling Chain Collapse at Infinite Dilution in Θ-Solvent. Confronted by experimental limitations that precluded direct observation of the effects of intramolecular associations on individual chain dimensions, we developed a model of single-chain statistics at infinite dilution in Θ-solvent. Consider a polymer chain containing N monomers and f stickers separated by $l = N/(f - 1)$ monomers (meaning there are stickers at each chain end), with pairwise association of the stickers of energy

Table 4. Normalized Apparent Hydrodynamic Radii of Functionalized 1250 kg/mol 1,4-Polybutadiene Chains in Jet-A and Chlorododecane (CDD)[a]

	0.2% A[b]		0.3% A[b]		0.4% A[b]		0.6% A[b]	
c (by wt, in ppm)	Jet-A	CDD	Jet-A	CDD	Jet-A	CDD	Jet-A	CDD
500	1.02		1.07	0.95	1.07	1.02	1.06	0.91
900	1.03		1.10	0.99	1.12	1.07	1.10	0.96
1500	1.10		1.21	1.05	1.25	1.15	1.23	1.07
2500≈c^*	1.14		1.27	1.14	1.32	1.30	1.29	1.23

[a] Measurements were carried out at 25 °C, and results are reported as normalized hydrodynamic radii relative to the unfunctionalized chains (for which at 500 ppm R_h = 25.2 nm in Jet-A and 47.9 nm in CDD). The standard deviation of measurements was <2% of the measured value in all cases. [b] The degree of functionalization with 3-mercaptopropionic acid, as indicated in Table 1.

εkT. Time-average properties of such a chain were calculated by tracking the evolution of the chain through a large number of bond-forming and bond-breaking events. This stochastic process corresponds to a semi-Markov chain,[29] such that a state of the process (corresponding to a state of the polymer chain) is fully specified by identifying which pairs of stickers form bonds, and the chain transitions from one state to the next by either breaking a bond or forming a new bond. Stickers are indexed from 1 to f (Figure A.2 in Supporting Information); the position of sticker m relative to sticker n is $\vec{R}_n - \vec{R}_m$, and the number of monomers in the shortest connected path between stickers n and m is $L_{n,m}$. Because the strand corresponding to the shortest path between stickers is free to adopt any configuration and therefore has Gaussian statistics in Θ-solvent, the dimensionless root-mean-square end-to-end (1-to-f) distance for any given state is approximately

$$\sqrt{\langle R^2/b^2 \rangle} = L_{1,f}^{1/2} \tag{3}$$

where b is the monomer Kuhn length. The dimensionless radius of gyration of the chain in any specific state is

$$\sqrt{\left\langle \frac{R_g^2}{b^2} \right\rangle} = \frac{1}{fb}\left(\sum_{n=1}^{f} \sum_{m=n}^{f} \langle (\vec{R}_n - \vec{R}_m)^2 \rangle \right)^{1/2} = \frac{1}{f}\left(\sum_{n=1}^{f} \sum_{m=n}^{f} L_{n,m} \right)^{1/2} \tag{4}$$

Averaging over a large number of successive states and accounting for the time spent in each state yields the time-average properties, such as the average size of the chain. A full description of the model is given in the Supporting Information.

Computer simulations according to the above model allowed us to quantify the effects of bond strength (Figure 7), degree of functionalization (Figure 8), and chain length (Figure 9) on chain configuration. In addition to overall measures of coil size (chain end-to-end distance and radius of gyration), we examined the fraction of stickers that are paired (*fps*) and the average spacing between paired stickers (*asps* = $\langle |p - p'| \rangle$, where p and p' are the indexes of stickers involved in pairs; refer to Figure A.2 of Supporting Information). Model predictions show that intrachain associations reduce both the end-to-end distance and the radius of gyration (Figures 7−9), with the end-to-end distance decreasing more strongly. The reduction in coil dimensions with increasing strength of association arises from two effects: an increase in the fraction of stickers that are paired and an increase in the fraction of "bonds" that occur between stickers that are widely separated along the backbone (Figure 7). Interestingly, the decrease of chain size with increasing extent of functionalization corresponds to remarkably straight lines on a log-normal plot (Figure 8). In other words, we observe that $R_{N,f} - R_{N,f=0} \sim \log(f)$, consistent with the expectation that the incremental extent of chain collapse with an incremental increase

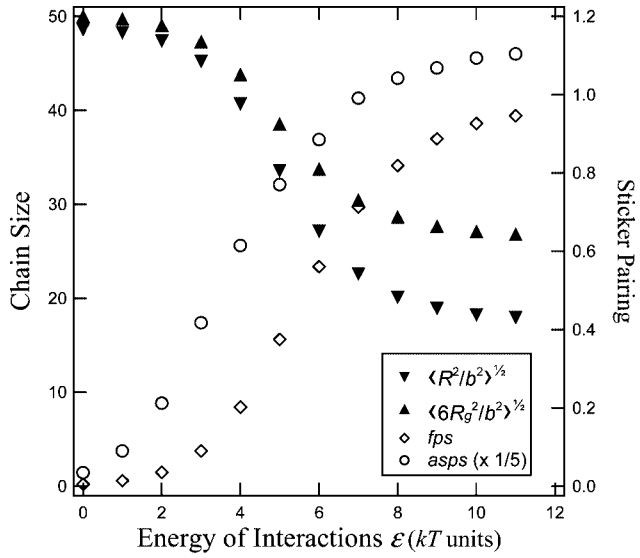

Figure 7. Simulation results of the end-to-end distance R, radius of gyration R_g, fraction of stickers paired (*fps*), and average spacing between paired stickers (*asps*, refer to text), as a function of energy of interaction εkT for a chain with $f = 25$ stickers and $l = 100$ monomers between stickers. The bond volume was taken to be $V_b = b^3$, and the time evolution of the chain was tracked over 2×10^5 bond-breaking or bond-forming events.

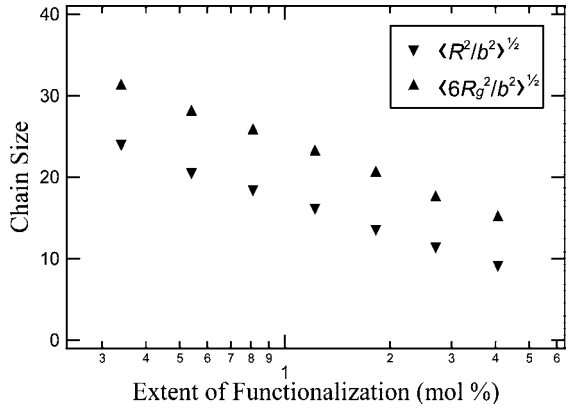

Figure 8. Simulation results of the end-to-end distance R and radius of gyration R_g as a function of the fraction of monomers bearing stickers (in mol %) for a chain with $N = 1500$ monomers at fixed energy of interaction $10kT$. The bond volume was taken to be $V_b = b^3$, and the time evolution of the chain was tracked over 4×10^4 bond-breaking or bond-forming events.

in f sharply declines as the chain becomes more compact (at higher degrees of functionalization). Finally, the increase in chain size upon increasing N at fixed l and ε does not follow a power law (Figure 9), meaning that the chains do not behave as fractals. Given that fractal (or self-similar) behavior requires that the configuration of any chain segment be independent of other segments of the molecule, this last result is not unexpected. The results of Figure 9 reveal that as a consequence of interactions with stickers on neighboring or distant segments, a polymer strand of given f, N (at fixed l) is more collapsed if it is part of a longer chain.

Elasticity and Mist Suppression—Drop Impact Experiments. The effect of self-associating stickers on solution elasticity and drop breakup in very dilute solutions is manifested in drop impact experiments (Figure 10). For comparison, 4200 kg/mol PIB at 180 ppm in Jet-A promotes the formation of fluid filaments which completely suppress the ejection of satellite droplets (Figure 10a), in sharp contrast to the rapid fragmentation

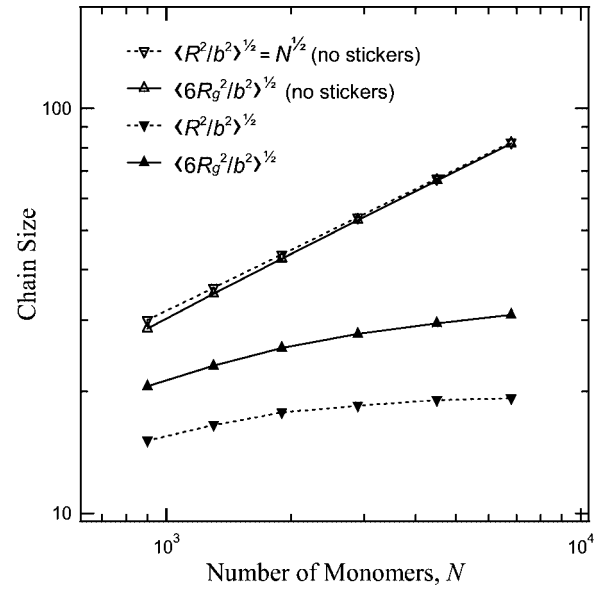

Figure 9. Simulation results of the end-to-end distance R and radius of gyration R_g as a function of chain length for a chain at fixed $l = 100$ and fixed energy of interaction $10kT$ (under these conditions the stickers spend the majority of their time in pairs). Open symbols correspond to chain size, calculated using eqs 3 and 4, for chains of matched length without stickers. The bond volume was taken to be $V_b = b^3$, and the time evolution of the chain was tracked over 10^5 bond-breaking or bond-forming events.

of ejected fluid in the absence of polymer (Figure 1a). Results for 1250kPB prepolymer at the same concentration (Figure 10b) reveal the pronounced effect of chain length on polymer elasticity: in contrast to the 4200 kg/mol PIB solution, there is more splashing of fluid upon impact, followed by rapid breakup of the ejected fluid. Nevertheless, the 1250kPB chains display sufficient elasticity to visibly hinder the necking and pinching processes involved in the breakup of individual droplets: filaments that form between beads of fluid survive for ~2 ms (Figure 10b). The ability of 1250kPB to hinder drop breakup is reduced by incorporation of carboxylic acid side groups at random positions along the chains, evidenced by a decrease in the lifetimes of fluid filaments for 1250kPB0.3A and 1250kPB0.6A solutions to 1.5 and 1 ms, respectively (Figure 10c,d).

Suppression of breakup was enhanced significantly by increasing the polymer concentration (Figure 11): at 450 ppm, the lifetimes of fluid filaments were 2.5, 2.5, and 2 ms for solutions of 1250kPB, 1250kPB0.3A, and 1250kPB0.6A, respectively. It is interesting to note that, while stickers bring no improvement still, the deleterious effects of intramolecular associations observed for 0.3% and 0.6% functionalization at 180 ppm are lessened at 450 ppm. This observation begs for comparison of solution elasticity and extensional viscosity at, and above, the overlap concentration. Unfortunately, complete suppression of fluid breakup occurred for all 1250kPB solutions at polymer concentrations of c^* or more. Characterization of fluid breakup at the overlap concentration and in the semidilute regime required spray experiments and capillary breakup experiments.

Elasticity and Mist Suppression—Spray and CaBER Experiments. Spray experiments for 1250kPB at c^* (2500 ppm by wt in Jet-A) revealed that 0.2−0.6 mol % of carboxylic acid stickers do not shift droplet size to higher values during atomization of the fuel (Figure 12). This simple qualitative experiment successfully detects mist suppression by 4200 kg/mol PIB (Figure 1b). In view of the pronounced increase in drop size as the concentration of 4200 kg/mol PIB is increased

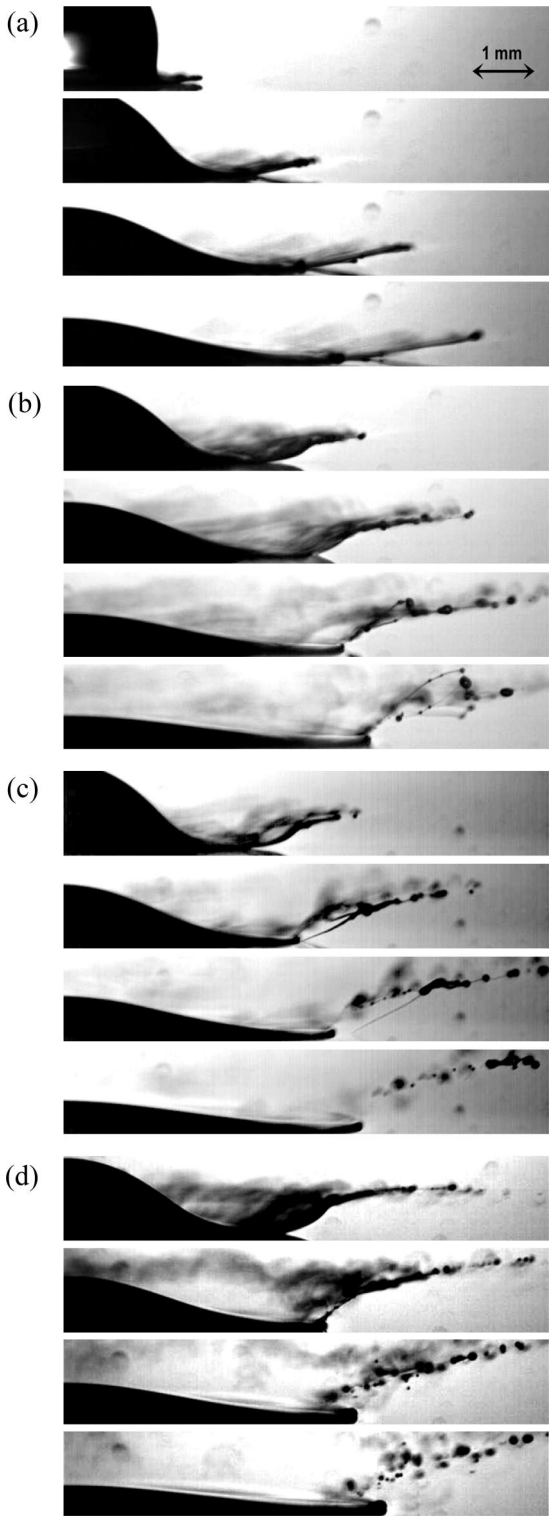

Figure 10. High-speed imaging of drop breakup of polymer solutions at 180 ppm by wt in Jet-A: (a) 4200 kg/mol linear, nonassociating polyisobutylene chains; (b) 1250 kg/mol linear, unfunctionalized 1,4-polybutadiene chains; (c) 1250kPB0.3A chains; and (d) 1250kPB0.6A chains (refer to Table 1). For 4200kPIB, satellite droplets were never fully ejected; on the other hand, all visible fluid filaments connecting "beads" of fluid together had broken 2, 1.5, and 1 ms after impact for solutions b, c, and d, respectively. The interval between frames is 0.25 ms in all cases.

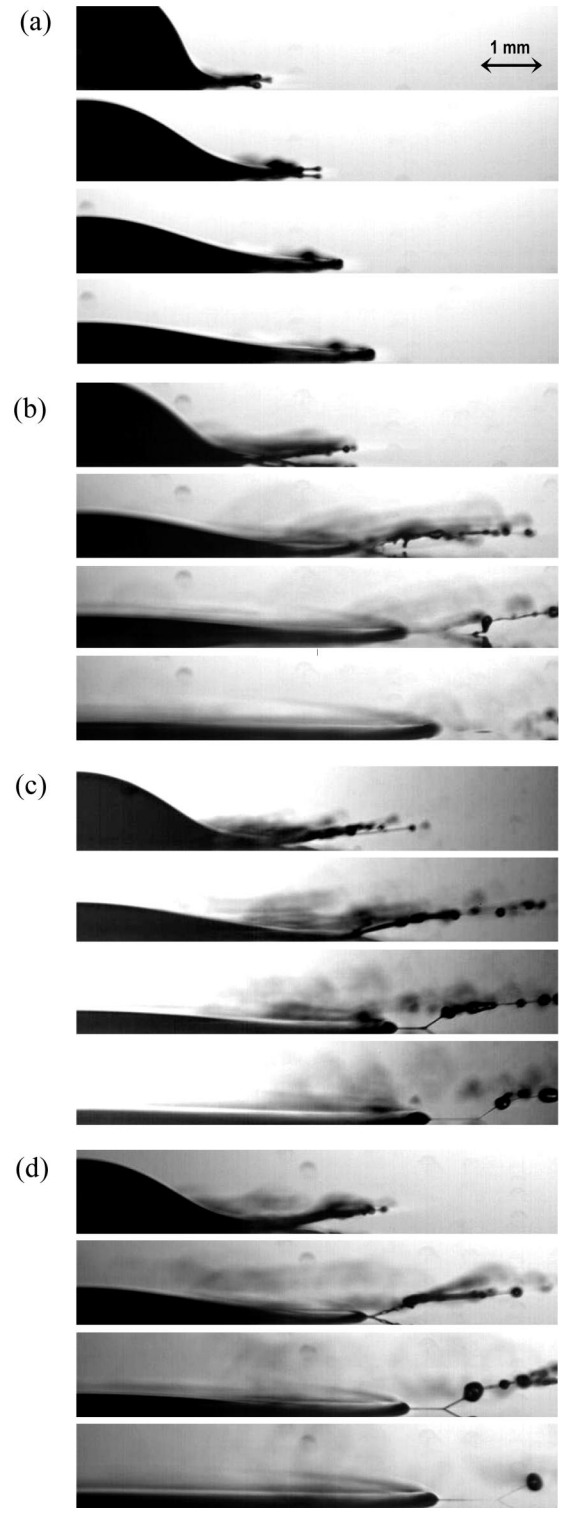

Figure 11. High-speed imaging of drop breakup of polymer solutions at 450 ppm by wt in Jet-A: (a) 4200 kg/mol linear, nonassociating polyisobutylene chains; (b) 1250 kg/mol linear, unfunctionalized 1,4-polybutadiene chains; (c) 1250kPB0.3A chains; and (d) 1250kPB0.6A chains (refer to Table 1). For 4200kPIB, there is nearly complete suppression of breakup, without formation of satellite droplets; on the other hand, all visible fluid filaments connecting "beads" of fluid together had broken 2.5, 2.5, and 2 ms after impact for solutions b, c, and d, respectively. The interval between frames is 0.5 ms in all cases.

from 50 to 200 ppm, the drop size is remarkably insensitive to the addition of stickers to 1250kPB. The slight effects that stickers have are unfavorable for mist suppression: the size of droplets appears to decrease as functionalization increases from 0 to 0.3 mol % and only recovers to be similar to that for the unmodified polymer as functionalization is increased further to 0.6 mol % (the solubility limit).

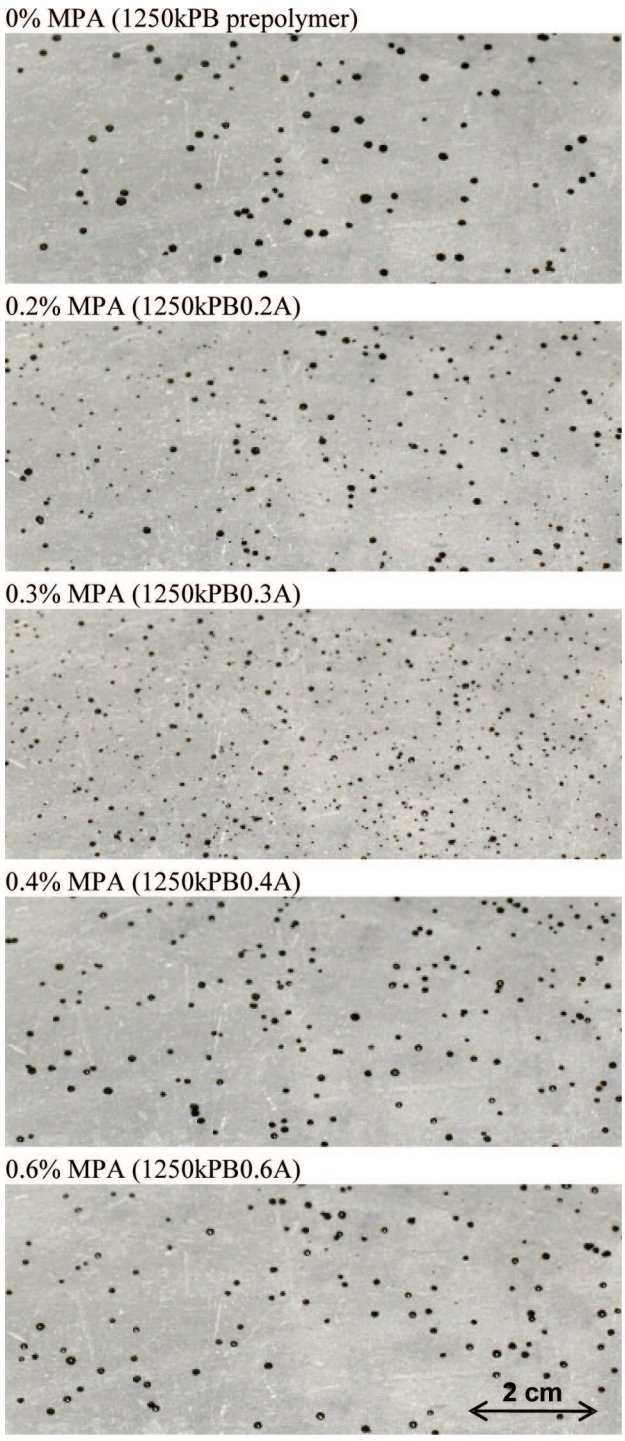

Figure 12. Spray patterns of solutions of 1250 kg/mol 1,4-polybutadiene chains (refer to Table 1) at 2500 ppm by weight in Jet-A as a function of increasing mercaptopropionic acid content.

To proceed beyond qualitative observations, quantitative measurements of extensional viscosity and relaxation time were attempted using capillary breakup rheometry. Unfortunately, the minimum concentration that gave adequate solution elasticity was 1.5 wt % in Jet-A solvent for the 1250 kg/mol PB series (corresponding to $c = 6c^*$). CaBER results for solutions of 1250kPB0.3A and 1250kPB0.6A polymers show that, at 1.5 wt % polymer in Jet-A, associations caused modest (60−200%) increases relative to 1250kPB in the following parameters: the breakup time of filaments, the solution's relaxation time, and the solution's apparent extensional viscosity (Figure 13 and Figure A.1 of the Supporting Information). Relative to shear

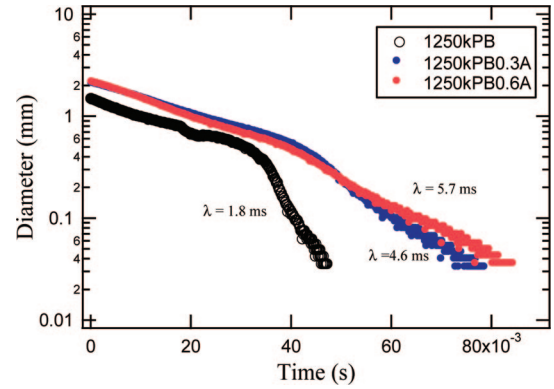

Figure 13. Time evolution of filament diameter during capillary breakup experiments for 1250kPB, 1250kPB0.3A, and 1250kPB0.6A polymers at 1.5 wt % total polymer content in Jet-A (corresponding to $c = 6c^*$ for 1250kPB prepolymer). All tests were performed with 8 mm diameter plates, at initial and final aspect ratios of 1.0 and 2.5, respectively. Solution shear viscosities were 48, 83, and 95 mPa·s for the 1250kPB, 1250kPB0.3A, and 1250kPB0.6A solutions, respectively. The characteristic relaxation times of the solutions, determined from the slope of the exponential decay of the filament diameter vs time, are represented in the figure.

viscosity, the increases in relaxation time[30] compared to the prepolymer solution were only 50% for 1250kPB0.3A and 60% for 1250kPB0.6A. This amounts to considerably smaller effects of stickers on extensional viscosity than reported behavior for similar systems (Figure 14c; refer to Discussion below).

Discussion

To obtain a fundamental understanding of the behavior of self-associating polymers, it proved useful to synthesize homologous series of narrow-disperse chains of controlled molecular properties. Polymer analogous synthesis allowed chains of matched length and distribution to be compared with and without "stickers". Given that the effect of stickers proved to be surprisingly small, it could have been obscured by batch-to-batch variation in chain length or in chain length distribution if individually synthesized copolymers had been compared instead of functionalized derivatives of a given prepolymer. The effects of carboxylic acid side groups (pairwise "stickers") on rheological behavior were investigated as a function of number density of side groups, polymer concentration, chain length, and solvent polarity.

Low-Concentration Solutions (Dilute and Unentangled Semidilute). In contrast to the extensive literature on polymers that associate in solution through many-body interactions (such as ionic interactions in low-polarity solvents or hydrophobic interactions in aqueous media), the literature on pairwise associating stickers is sparse, particularly in relation to the low-concentration regime pertinent, for instance, to fuel additives. Indeed, there are only two bodies of work that we have found focusing on dilute and semidilute solutions of long, flexible polymer bearing pairwise, self-associating stickers: studies of ICI's FM-9 polymer[32,33] and studies of Exxon's polyoctene copolymers.[10,11,28] Our experiments confirmed the reduction in shear viscosity (Figure 4) reported for dilute solutions ($c < c^*$ in Figure 14a). We found that the reduction of shear viscosity was accompanied by a reduction in the apparent extensional viscosity, as seen in drop breakup experiments (Figures 10 and 11). These behaviors are a consequence of the previously recognized phenomenon[10,28] of chain collapse driven by intramolecular associations in dilute solutions. Computations confirm that for chains of $\sim 10^4$ Kuhn monomers, containing ~ 1 mol % side groups that associate pairwise with energy

$\sim 10kT$ (closely matching our 1250kPB0.6A polymer in DD), chain collapse is severe (Figure 9).

A number of salient rheological characteristics attributed to pairwise stickers in the prior literature are conspicuously absent in the present systems. Expected features include an extremely nonlinear increase in viscosity with concentration in the semidilute unentangled regime, pronounced shear thickening, and strongly enhanced extensional viscosity (Figure 14). Discrepancies may originate in differences in molecular structure, since the earlier studies examine much longer chains or much greater sticker density.[34] Perhaps other regimes of behavior are found in other regions of the parameter space. For example, the hypothesis that chains "zip" together into bundles that confer shear thickening may apply only to high sticker densities.[35]Alternatively, incipient phase separation may have given rise to some of the prior rheological signatures attributed to pairwise stickers.[36]

Our results for solutions of concentration $\geq c^*$ uncover physical phenomena overlooked in the prior literature. We observed that at c^* adding stickers *reduces* both shear viscosity (Table 3, Figure 4) and mist suppression (indicative of a reduction in extensional viscosity; Figure 12). For $c > c^*$, we observed that the effects of stickers on both shear and apparent extensional viscosity (Figure 4, Figure A.1 in Supporting Information) were remarkably weak in comparison to those shown in Figure 14. These results reveal that the effects of chain collapse due to intrachain pairing are important beyond the dilute regime. This physical insight was lacking in the prior literature, according to which intermolecular interactions are believed to dominate solution behavior above c^*. The implications for mist control of aviation fuel are that self-associating polymers with acceptable shear degradation and solubility in the fuel are not superior to their nonassociating analogues even at concentrations several times above c^*.

Entangled Solutions. The viscosity vs concentration results we obtained for entangled solutions of 510 kg/mol PB chains (Figure 4) were in good agreement with the only experimental body of work reporting on the dynamics of solutions of pairwise associating polymer: Stadler and de Lucca Freitas[37] modified anionically synthesized PB with hydrogen-bonding 1,2,4-triazolidine-3,5-dione side groups and reported a $\eta \sim \phi^6$ concentration dependence of zero-shear viscosity for squalene solutions of 1% modified chains of 2×10^5 g/mol, over almost 1 decade in concentration corresponding to $0.1 < \phi < 1$. Note that this concentration dependence is identical to that which we observed for 510kPB1.8A at volume fractions $\phi > 0.08$ in CDD (Figure 4). Given the $\eta \sim \phi^{5.3}$ relationship measured for the unfunctionalized 510kPB prepolymer, this observed increase in the exponent of the concentration dependence of viscosity due to stickers seems very moderate.

The measured effect of self-associating, pairwise polymer interactions on solution viscosity is much weaker than anticipated based on theoretical literature models of such systems. For example, Rubinstein and Semenov[23−25] predicted scaling exponents up to 8.5 in a concentration regime corresponding to a transition from predominantly intramolecular to predominantly intermolecular interactions (Figure 15, refer to footnote 38 for a brief description of the model). For 510 kg/mol PB chains with carboxylic acid content up to 1.8 mol %, the observed shape of the viscosity vs concentration curves was strikingly similar to that of the unmodified polymer, in contrast to model predictions (compare Figures 4 and 15).

Why the differences? First, it is difficult to satisfy the assumptions of Rubinstein and Semenov's model for homogeneous solutions, particularly in terms of the strength of associations for pairwise stickers. Second, the theory neglects the effect

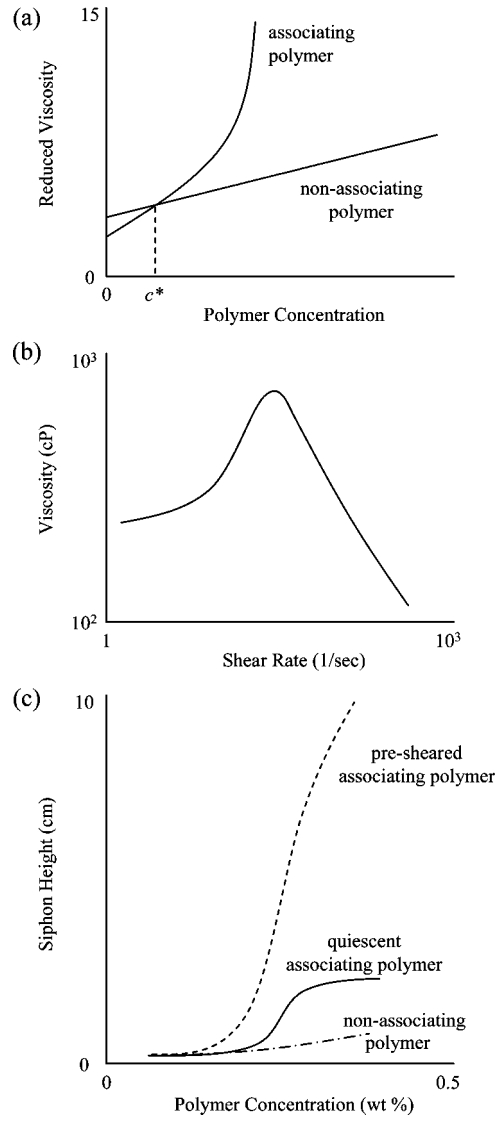

Figure 14. Prior understanding of the physical properties of solutions of self-associating polymer of low concentrations, according to Schulz et al.[28] Siphon height is a measure of extensional viscosity.[31] (Redrawn from ref 28.)

of intramolecular interactions on the chain statistics. We discuss these two aspects in turn.

Satisfying Model Assumptions. Very little existing literature deals with solutions of linear polymers associating via binary interactions. In fact, for lack of a better choice, Rubinstein and Semenov[24] were compelled to compare their model predictions with experimental results of polymer systems interacting through many-body (rather than pairwise) association of hydrophobic groups in aqueous solutions. Given the binary nature of carboxylic acid associations, our use of synthetic methods enabling control of polymer functionalization at fixed chain length led to materials that appear particularly well-suited to test Rubinstein and Semenov's model predictions.

Despite of our best efforts in selecting the "stickers", the structure of the backbone, and the set of solvents, our system is not an exact realization of their model. Regarding solvent quality and strengths of interactions, two key assumptions[24] underpin the predicted concentration dependence of the viscosity of entangled reversible networks (Figure 15): the solvent is good (monomer excluded volume parameter v of order b^3), and associations are strong (such that $e^{\varepsilon} > l^{2.225}$). Our best estimate of the association energy for dimerization of carboxylic acids in CDD[39] corresponds to $\varepsilon \approx 8-10$. Assuming a Kuhn monomer

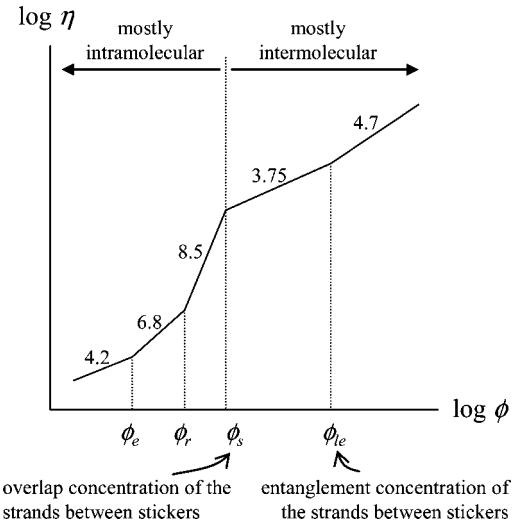

Figure 15. Predictions of Rubinstein and Semenov's model[24] for the concentration dependence of the viscosity of entangled reversible networks in good solvent. (Redrawn from ref 24. Refer to footnote 38 for identification of the crossover concentrations.) The numbers above each line segment indicate the predicted scaling exponent.

of molar mass ~ 100 g/mol, the distances between stickers are $l \sim 180$, 55, and 30 Kuhn monomers for the present 0.3%, 1%, and 1.8% functionalized chains. Thus, "strong association" is expected to hold in CDD for 510kPB1.0A and 510kPB1.8A but is questionable for 510kPB0.3A. Further, our best estimate of the solvent quality for 510kPB chains in CDD[40] corresponds to $v/b^3 \sim 0.2$ or $\chi \sim 0.4$ (in accord with measured χ values for PB in shorter chloroalkanes reported by Alessi et al.).[22] Because Rubinstein and Semenov treat scaling behavior without knowledge of the prefactors, it is difficult to know from the above estimates of v/b^3 and ε whether or not our system fully satisfies the model requirements of "good solvent" and "strong interactions".

In practice, the "good solvent" and "strong pairwise associations" assumptions tend to be incompatible. Hydrogen-bonding systems model binary associations; however, their strengths of interaction are greatest in very nonpolar solvents such as *n*-alkanes, which are marginal solvents for all common polymers. On the other hand, efforts to satisfy the assumption of good solvent by using, for instance, chlorinated hydrocarbons or aromatic solvents compromise the strengths of hydrogen bond interactions. The relationship between the "good solvent" and "strong associations" criteria is further complicated by solvent−sticker interactions: Quantitative pairing of the stickers in a system requires low values of l and high values of ε, meaning high levels of functionalization with stickers exhibiting very favorable sticker−sticker interactions and, unfortunately, unfavorable sticker−solvent interactions. In this case, phase separation of the functional chains driven by adverse solvent−"sticker" interactions tends to occur.

Role of Intrachain Associations. The effect of chain collapse even above c^*, unnoticed in previous experimental work, was also overlooked in theoretical descriptions of self-associating polymer systems. Specifically, Rubinstein and Semenov's theory does not account for the effects of intramolecular bonds on the chains statistics. Intrachain associations cause polymer molecules to collapse onto themselves, even at concentrations $\gg c^*$, so that expressions for segment sizes and relaxation times that are applicable to linear chains without stickers no longer hold for self-associating polymer molecules. However, Rubinstein and Semenov did not include corrections to expressions of chain size R, correlation length ξ, number of monomers per correlation blob g, Zimm time of correlation blobs, tube length $a(\phi)$, etc. Calculations of chains collapse (Figures 7−9) show that changes in polymer configuration due to intrachain associations are substantial, especially for long chains and strong associations.

Conclusion

The results of this study challenge the pre-existing understanding of the rheology of self-associating polymers (Figures 14 and 15) and suggest that previously accepted assertions regarding the effects of pairwise stickers on the rheology of polymer solutions deserve re-evaluation. Properly controlled studies that compare functionalized and unmodified polymer homologues of matched, well-defined length using light scattering and rheological characterization provide valuable tests of prior beliefs.

For 510 and 1250 kg/mol PB chains of low polydispersity, we find that incorporation of carboxylic acid side groups results in a strong tendency for phase separation. For homogeneous solutions, enhancements in shear and extensional viscosity due to stickers are relatively small, even at polymer concentrations $\gg c^*$, in contrast with prior expectations. Our results reveal that the effects of chain collapse due to intrachain pairing are important beyond the dilute regime—behavior unaccounted for in earlier experimental and theoretical studies. The implications for mist control of aviation fuel are that self-associating polymers of acceptable solubility in the fuel are *not* superior to nonassociating polymers even at concentrations several times c^*. Therefore, alternative strategies to improve antimisting using associative polymers are needed.

Acknowledgment. Funding for this research was provided by the FAA and NASA, the Caltech Milliken Foundation, and the Caltech Gates Grubstake Fund. We thank Dr. Steven Smith of Procter and Gamble Company for supplying the 1,2-PB precursor materials and Dr. Suneel Kunamaneni for contributing the ideas that initiated the direction of this work.

Supporting Information Available: Method for the determination of the acid content of functionalized polymer; extensional viscosity results of select solutions; numerical approach for the study of the chain statistics of self-associating chains at infinite dilution in Θ-solvent. This material is available free of charge via the Internet at http://pubs.acs.org.

References and Notes

(1) Anna, S. L.; McKinley, G. H. *J. Rheol.* **2001**, *45* (1), 115–138.
(2) Chao, K. K.; Child, C. A.; Grens, E. A.; Williams, M. C. *AIChE J.* **1984**, *30* (1), 111–120.
(3) Christanti, Y.; Walker, L. M. *J. Rheol.* **2002**, *46* (3), 733–748.
(4) Smolinski, J. M.; Gulari, E.; Manke, C. W. *AIChE J.* **1996**, *42* (5), 1201–1212.
(5) Oliver, D. R.; Bakhtiyarov, S. I. *J. Non-Newtonian Fluid Mech.* **1983**, *12* (1), 113–118.
(6) Note that mist-control ability increases strongly with both increasing molecular weight and concentration.
(7) Motier, J. F. Hydrocarbon fuels containing antimisting agents. European Patent 0177649, **1986**.
(8) Brostow, W. *Polymer* **1983**, *24* (5), 631–638.
(9) Knight, J. Antimisting additives for aviation fuels. United States Patent 4,396,398, **1983**.
(10) Kowalik, R. M.; Duvdevani, I.; Peiffer, D. G.; Lundberg, R. D.; Kitano, K.; Schulz, D. N. *J. Non-Newtonian Fluid Mech.* **1987**, *24* (1), 1–10.
(11) Schulz, D. N.; Kitano, K.; Duvdevani, I.; Kowalik, R. M.; Eckert, J. A. *ACS Symp. Ser.* **1991**, *462*, 176–189.

(12) Association of carboxylic acids is pairwise and noncomplementary (referring to pairing of identical groups, as opposed to paring of donor−acceptor complementary groups) via formation of two O--HO hydrogen bonds (Jones, M. In *Organic Chemistry*, W. W. Norton & Co., Inc.: New York, 2nd ed.; 2000; p 890). These interactions prevail both in the gas phase (Smith, M. B.; March, J. In *March's Advanced Organic Chemistry. Reactions, Mechanisms, and Structure*, 5th ed.; John Wiley & Sons: New York, 2001; p 99) and in solution when the solvent does not disrupt hydrogen bonding (Davis, M. M., *Acid-Base Behavior in Aprotic Organic Solvents*; U.S. National Bureau of Standards: Washington, DC., 1968).
(13) Justynska, J.; Hordyjewicz, Z.; Schlaad, H. *Polymer* **2005**, *46* (26), 12057–12064.
(14) Justynska, J.; Hordyjewicz, Z.; Schlaad, H. *Macromol. Symp.* **2006**, *240*, 41–46.
(15) Rodd, L. E.; Scott, T. P.; Cooper-White, J. J.; McKinley, G. H. *Appl. Rheol.* **2005**, *15* (1), 12–27.
(16) Bathel, B. F.; Stephen, N.; Johnson, L.; Ratner, A.; Huisenga, M. *AIAA J.* **2007**, *45* (7), 1725–1733.
(17) Standard methods to measure particle size of sprays and aerosols predominantly rely of analysis of laser diffraction patterns (where the intensity of light scattered by spray particles is measured as a function of scattering angle). In addition to the usual difficulties of mist characterization, our efforts were complicated by the challenge of handling toxic vapors. In our limited attempts to characterize drop size distribution using a simple homemade, properly vented laser diffraction apparatus, air flow added to the variability in the position of the cloud of droplets, and highly variable scattering patterns resulted. For the polymer materials discussed here, photographs of the spray patterns on the bench surface (as shown in Figures 1and 12) provided sufficient information for our purposes. Future researchers may wish to implement light scattering in conjunction with a laminar flow optical chamber to convect and then exhaust the mist.
(18) David, R. L. A.; Kornfield, J. A. *Macromolecules* **2008**, *41* (4), 1151–1161.
(19) The following confounding effects precluded interpretation of the precise elution time of the GPC peaks, leading us to omit the corresponding values of M_w from Table 1: (i) the calibration curve of M_w vs elution time for polystyrene standards was extremely steep for $M_w > 500$ kg/mol; therefore, the small variability (5−10 s) in the instrument injection transient produced a significant scatter in the inferred M_w; (ii) addition of functional groups shifts the elution time for a fixed polymer molar mass, as demonstrated in a prior publication (see Table 1 of ref 18); and (iii) pendent vinyl groups can become sites for cross-linking (making the 510 kg/mol 1,2-PB series more susceptible than the 1250 kg/mol 1,4-PB series), which might truly increase M_w and result in a shift in elution time. On the other hand, PDI measurements were fairly insensitive to the precise value of the elution time and therefore significantly more reliable. The shape of the GPC curves for aged polymer (Figure 3) suggests that changes in M_n upon aging were negligible relative to the changes in M_w. Consequently, we suggest that reasonable estimates of M_w for the polymers in Table 1might be obtained by multiplying the reported PDI value of each polymer by the M_n of the appropriate prepolymer (i.e., 510/1.15 kg/mol = 445 kg/mol for 510kPB and 1250/1.09 kg/mol = 1145 kg/mol for 1250kPB).
(20) That is, we are expecting that the changes in conformation, hydrodynamic volume, and specific viscosity resulting from the cyclization of 0.2−2% of monomers into isolated (non-polycyclic) rings are small (see ref 18).
(21) Davis, M. M. In *Acid-Base Behavior in Aprotic Organic Solvents*; U.S. National Bureau of Standards: Washington, DC., 1968; pp 31−37.
(22) Alessi, P.; Cortesi, A.; Sacomani, P.; Valles, E. *Macromolecules* **1993**, *26* (23), 6175–6179.
(23) Rubinstein, M.; Semenov, A. N. *Macromolecules* **1998**, *31* (4), 1386–1397.
(24) Rubinstein, M.; Semenov, A. N. *Macromolecules* **2001**, *34* (4), 1058–1068.
(25) Semenov, A. N.; Rubinstein, M. *Macromolecules* **1998**, *31* (4), 1373–1385.
(26) The overlap concentration of a segment of size N monomers scales with $N^{1-3\nu}$, where the fractal exponent is $\nu \approx 0.588$ in good solvent.
(27) $\eta_{sp} = 2.5\phi$ for noninteracting, rigid, spherical particles dispersed in a liquid medium, meaning that the particles' contribution to solution viscosity depends only their total volume fraction in solution ϕ and is independent of their size.
(28) Schulz, D. N.; Bock, J. *J. Macromol. Sci., Chem.* **1991**, *A28* (11−12), 1235–1243.
(29) A semi-Markov chain is a stochastic process that takes on a finite number of states, that moves from one state to the next according to transition probabilities P_{ij} (P_{ij} is the probability to transition from state i into state j), and such that the amount of time it spends in any state i, before proceeding to the next state, is a random variable with distribution T_i. When the time spent in every state is always 1, the semi-Markov process is just a Markov chain.
(30) I.e., we are comparing the ratios (solution relaxation time)/(solution shear viscosity).
(31) Peng, S. T. J.; Landel, R. F. *J. Appl. Phys.* **1976**, *47* (10), 4255–4260.
(32) Peng, S. T. J.; Landel, R. F. *J. Appl. Phys.* **1981**, *52* (10), 5988–5993.
(33) Peng, S. T. J.; Landel, R. F. *J. Non-Newtonian Fluid Mech.* **1983**, *12* (1), 95–111.
(34) On the one hand, the polyoctene copolymers prepared by Schulz (refs 10 and 11) had $M_n \sim (2-5) \times 10^6$ g/mol, so M_w up to $(10-20) \times 10^6$ g/mol (the Zeigler−Natta method of polymerization used in the preparation of the materials characteristically results in very high product polydispersity). On the other hand, the carboxylic acid content of FM-9 was 5−7 wt % methacrylic acid, according to the preferred composition divulged in the patent literature (ref 9).
(35) It has been suggested that interpolymer association can be favored by flow, causing chains to adopt more open/extended conformations with a preferred alignment. When stickers are closely spaced along the chain, it is hypothesized that cooperative "zipping of stretched chains" can occur. This scenario has been invoked to explain shear thickening (Kjoniksen, A. L.; Hiorth, M.; Nystrom, B. *Eur. Polym. J.* **2005**, *41* (4)), 761−770)as well as improved drag reduction and resistance to shear degradation (Malik, S.; Mashelkar, R. A. *Chem. Eng. Sci.* **1995**, *50* (1)), 105−116).
(36) Given the importance of solvent effects and the prevalence of phase separation that we observed, it is striking that the previous studies (refs 10, 11, 28, 32, and 33) do not provide solubility data. In view of the present results, we deduce that the high degree of functionalization in FM-9 would drive phase separation of the solutions; indeed, the patent literature describes the solutions as "hazy" and "opalescent" (ref 9). As a result of the limited amount of experimental detail in the prior literature, it is impossible to determine which rheological features pertain to microscopically homogeneous solutions and which correspond to phase-separated mixtures.
(37) Stadler, R.; Freitas, L. D. *Makromol. Chem., Macromol. Symp.* **1989**, *26*, 451–457.
(38) Rubinstein and Semenov's model describes the static and dynamic properties of solutions of linear chains randomly functionalized with pairwise, self-associating groups. They assumed monodisperse chains of N Kuhn monomers, containing f stickers capable of forming pairwise associations of energy εkT, located at constant intervals (i.e., separated by $l = N/f$ monomers) along the entire chains. For entangled polymer chains with strongly associating stickers, above the gel point and in good solvent, the model predicts a rich cascade of scaling regimes in the concentration dependence of viscosity shown in Figure 15 (ref 24). Transitions from one regime to another are predicted to occur at the entanglement concentration ϕ_e, the overlap concentration of the strands between stickers ϕ_s, the entanglement concentration of the strands between stickers ϕ_{le}, and a crossover concentration ϕ_r above which the lifetime of bonds must be renormalized to account for reassociation of the same pair of separated stickers due to a shortage of free partners. Below ϕ_s, any sticker's closest partners in space are its neighbors on the same chain, so interactions are mostly intramolecular. The steep increase in viscosity with concentration between ϕ_e and ϕ_s corresponds to a transition from predominantly intramolecular to predominantly intermolecular pairing. For comparison, the concentration dependence of viscosity for linear, nonassociating chains is $\eta \sim \phi^{1.3}$ below ϕ_e and $\eta \sim \phi^{3.9}$ above ϕ_e according to de Gennes' reptation model. We note that the $\eta \sim \phi^{5.3}$ relationship which we observed above ϕ_e for unmodified PB is consistent with the well-known observation that the simple reptation model underestimates the value of the exponent for real chains (Rubinstein, M.; Colby, R. H. In *Polymer Physics*; Oxford University Press: New York, 2003; p 374).
(39) Obtained using published equilibrium constants of associations (Davis, M. M. In *Acid-Base Behavior in Aprotic Organic Solvents*; U.S. National Bureau of Standards: Washington, DC., 1968; pp 31−37).
(40) Obtained for 510kPB chains in CDD by rearrangement of the scaling relation $\phi^* \approx (b3/v)^{6\nu-3}N^{1-3\nu}$ (Rubinstein, M.; Colby, R. H. In *Polymer Physics*; Oxford University Press: New York, 2003; eq 5.19, p 176)using swelling exponent $\nu \approx 0.588$ and overlap concentration $\phi^* \cong 0.003$. In the above equation, v is the excluded volume parameter and b is the Kuhn monomer length. The number of Kuhn monomers N was estimated for chains of $M_w \sim 510$ kg/mol assuming Kuhn monomers of molecular weight ∼ 100 g/mol.

MA802058S